frontiers | Frontiers in Immunology

TYPE Original Research
PUBLISHED 15 September 2023
DOI 10.3389/fimmu.2023.1259612

OPEN ACCESS

EDITED BY
Sumra Abbasi,
National University of Medical Sciences (NUMS), Pakistan

REVIEWED BY
Angel Alejandro Oñate,
University of Concepcion, Chile
Fábio Mambelli Silva,
Federal University of Minas Gerais, Brazil
Mohammad Reza Rahbar,
Shiraz University of Medical Sciences, Iran

*CORRESPONDENCE
Zhiguang Ren
renzhiguang66@126.com
Asifullah Khan
asif@awkum.edu.pk
Saadullah Khattak
saadullah271@gmail.com

†These authors have contributed equally to this work

RECEIVED 16 July 2023
ACCEPTED 24 August 2023
PUBLISHED 15 September 2023

CITATION
Aiman S, Ahmad A, Khan AA, Alanazi AM, Samad A, Ali SL, Li C, Ren Z, Khan A and Khattak S (2023) Vaccinomics-based next-generation multi-epitope chimeric vaccine models prediction against *Leishmania tropica - a* hierarchical subtractive proteomics and immunoinformatics approach. *Front. Immunol.* 14:1259612. doi: 10.3389/fimmu.2023.1259612

Vaccinomics-based next-generation multi-epitope chimeric vaccine models prediction against *Leishmania tropica - a* hierarchical subtractive proteomics and immunoinformatics approach

Sara Aiman[1†], Abbas Ahmad[2†], Azmat Ali Khan[3], Amer M. Alanazi[3], Abdus Samad[4], Syed Luqman Ali[4], Chunhua Li[1], Zhiguang Ren[5*], Asifullah Khan[4*] and Saadullah Khattak[6*]

[1]Faculty of Environmental and Life Sciences, Beijing University of Technology, Beijing, China, [2]Department of Biotechnology, Abdul Wali Khan University Mardan, Mardan, Pakistan, [3]Pharmaceutical Biotechnology Laboratory, Department of Pharmaceutical Chemistry, College of Pharmacy, King Saud University, Riyadh, Saudi Arabia, [4]Department of Biochemistry, Abdul Wali Khan University Mardan (AWKUM), Mardan, Pakistan, [5]The First Affiliated Hospital, Henan University, Kaifeng, China, [6]Henan International Joint Laboratory for Nuclear Protein Regulation, School of Basic Medical Sciences, Henan University, Kaifeng, Henan, China

Leishmania tropica is a vector-borne parasitic protozoa that is the leading cause of leishmaniasis throughout the global tropics and subtropics. *L. tropica* is a multidrug-resistant parasite with a diverse set of serological, biochemical, and genomic features. There are currently no particular vaccines available to combat leishmaniasis. The present study prioritized potential vaccine candidate proteins of *L. tropica* using subtractive proteomics and vaccinomics approaches. These vaccine candidate proteins were downstream analyzed to predict B- and T-cell epitopes based on high antigenicity, non-allergenic, and non-toxic characteristics. The top-ranked overlapping MHC-I, MHC-II, and linear B-cell epitopes were prioritized for model vaccine designing. The lead epitopes were linked together by suitable linker sequences to design multi-epitope constructs. Immunogenic adjuvant sequences were incorporated at the N-terminus of the model vaccine constructs to enhance their immunological potential. Among different combinations of constructs, four vaccine designs were selected based on their physicochemical and immunological features. The tertiary structure models of the designed vaccine constructs were predicted and verified. The molecular docking and molecular dynamic (MD) simulation analyses indicated that the vaccine design V1 demonstrated robust and stable molecular interactions with toll-like receptor 4 (TLR4). The top-ranked vaccine construct model-IV demonstrated significant expressive capability in the *E. coli* expression system during *in-silico* restriction cloning analysis. The results of the present

study are intriguing; nevertheless, experimental bioassays are required to validate the efficacy of the predicted model chimeric vaccine.

KEYWORDS

leishmaniasis, reverse vaccinology, multi-epitope vaccine design, immunoinformatics, tropical diseases, vaccine design

1 Introduction

Leishmania tropica is a kinetoplastid parasitic protozoa and is the leading cause of leishmaniasis in tropical regions (1). The multidrug-resistant *L. tropica* is a serious health burden in the leishmaniasis endemic regions (2). *L. tropica* is a highly diverse species that covers most of Africa and Eurasia with a wide variety of serological, biochemical, and genomic characteristics (3). Leishmaniasis affects approximately 350 million people in 98 countries. Annually, around 12 million *leishmania* cases are reported worldwide, with approximately 2 to 2.5 million new occurrences. There are three main pathogenic types of leishmaniasis: mucocutaneous leishmaniasis (ML), cutaneous leishmaniasis (CL), and kala-azar (VL) (MCL). Among these CL is the most common type and affects the skin, causing scarring lesions. Approximately 1 to 1.5 million cases of CL are reported annually (4). VL is the deadliest type and is characterized by strong inflammatory reactions in the spleen and liver that may be fatal (4). A survey in 2018 revealed that more than 85% of new CL cases happened in different countries worldwide. Poverty, population shifts, malnutrition, poor hygiene, and immunocompromised conditions are the key risk factors associated with leishmaniasis (5).

The skin sores occur up to weeks to months at a site of female sandfly bite that can lead to severe conditions, if not treated. The clinical spectrum of leishmaniasis ranges from CL with varying degrees of lesion severity to VL. Several individuals have developed post-kala-azar leishmaniasis after medication, whereas nasopharyngeal MCL is uncommon (6). There is no commercially available vaccine that provides protection against leishmaniasis, although various studies have been conducted in this regard. Recombinant vaccines, such as Leish-F1, may provide some level of protection against natural infection (7). Recently, the ChAd63-KH DNA vaccine was reported promising in preventing *Leishmania* infection caused by *Leshmania donovani* and *Leshmania infantum*; however, this vaccine needs additional clinical evaluation (8). There are no reports available for commercial vaccines against *L. tropica*. Recent reports highlighted slight variations in antigen presentation as one of the possible reasons for vaccination failure in clinical trials (9).

The rapid genome sequencing technologies facilitated the availability of various pathogenic genomes. The accessibility to genome sequences of *Leishmania* species allows the researchers to detect genes involved in diseased pathways, leading to the determination of homologous antigenic peptides that could be used to develop a pan-*Leishmania* vaccine (10). A significant shift from traditional culture-based techniques to next-generation genome-based vaccine development approaches has emerged recently due to the advancement of the genomic era. It is based on genomic and immunological data to determine relevant antigenic peptides for the purpose of vaccine designing (11). The vaccine designed based on the proteome fragments of the parasite enables the vaccine to elicit humoral and cellular immune responses against the pathogen (12). The present study aimed to identify highly immunogenic B- and T-cell epitopes from lead vaccine candidate proteins to engineer a multi-peptide-based vaccine construct against *L. tropic* infection. The chimeric vaccine construct models were evaluated using immunoinformatics approaches to determine their immunogenic potential. Biophysical techniques were employed to determine structural dynamics and binding affinities of the top-ranked vaccine construct model with human immune-cell receptors.

2 Methodology

A step-wise methodological perspective of the present study is depicted in Figure 1.

2.1 Proteome sequences retrieval

Protein sequences for *L. tropica* were obtained from TriTrypDB-kinetoplastid informatics resource (https://tritrypdb.org/tritrypdb/app/) following a recently published study (13). Non-paralogous protein sequences were obtained based on a sequence similarity index threshold of 80% using the CD-HIT tool (14).

2.2 Identification of pathogen essential proteins

Non-redundant protein sequences were screened against the Database of Essential Genes (DEG) to identify key proteins essential for the cellular survival of the pathogen. DEG repository holds cellular essential genes from archaea, bacteria, and eukaryotes that have been experimentally verified (15). A custom database was created from essential genes of eukaryotic using the "makedb" executable of the standalone BLASTp program (16). The BLASTp parameters were set at an E-value cut-off of 10^{-4}, ≥100 bit score, and ≥ 35% query coverage and sequence identity.

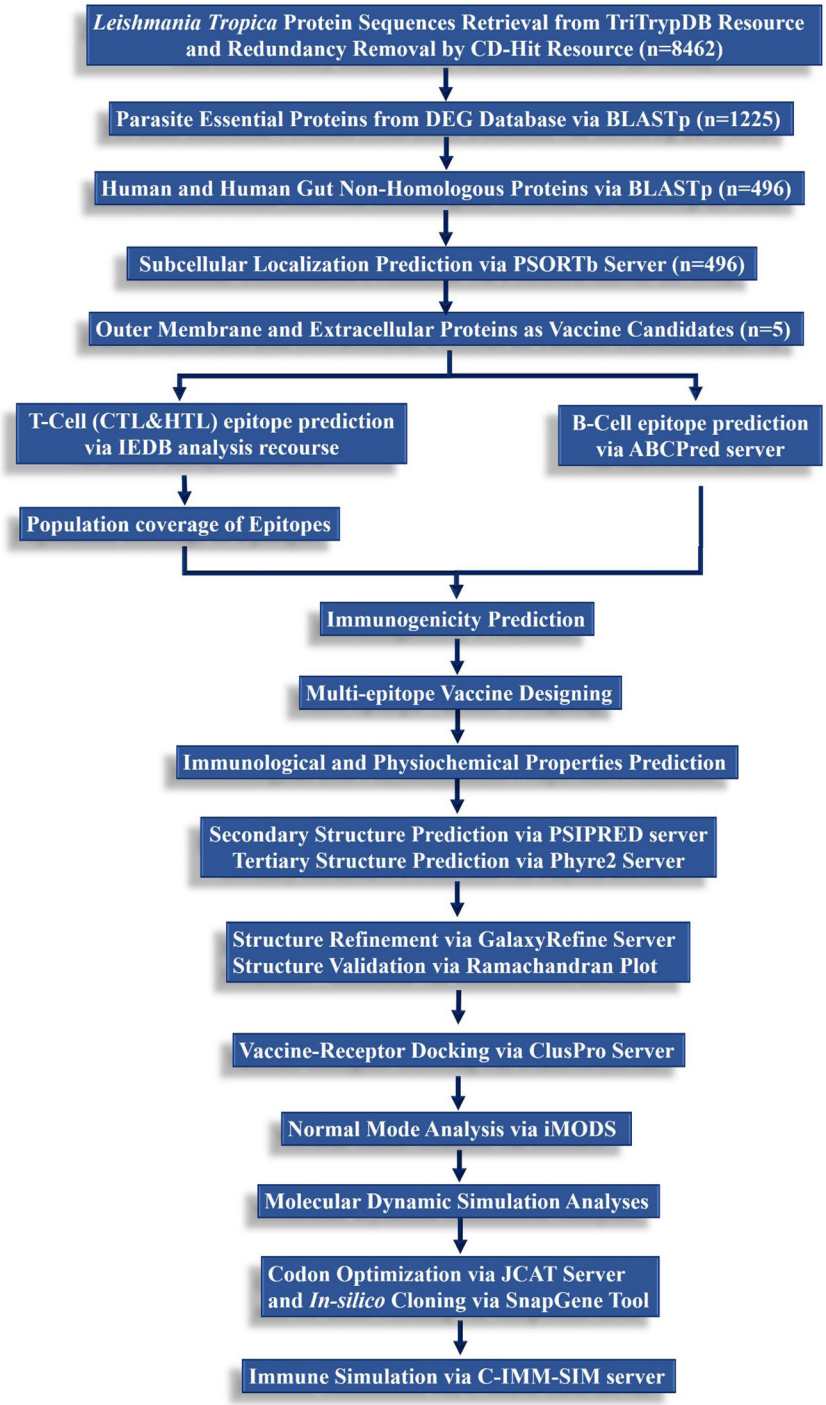

FIGURE 1
A hierarchical workflow of the present study following subtractive proteomics and reverse vaccinomics approaches to design a multi-peptide-based vaccine against *L. tropica*.

2.3 Identification of human host non-homologous proteins

The parasite-essential proteins were further subjected to BLASTp analysis against the human proteome (17) data, obtained from the NCBI database (18), to identify pathogen-essential proteins, non-homologous to host proteins. The resultant human non-homologous protein sequences of the pathogen were screened against human gut microbiota proteins (19). The BLASTp threshold criteria of bit score ≤100, sequence identity and query coverage of ≤35% and E-value cut-off of 10^{-4} were followed during this step.

2.4 Subcellular localization and vaccine candidates' selection

Parasite proteins were further subjected to subcellular localization using the PSORTb v.3.0.2 web server (20). The outer membrane and extracellular proteins were prioritized for downstream investigation.

2.5 Prediction of CTLs, HTLs, and linear B-cell epitopes

The surface topology of the prioritized proteins is crucial for predicting the immunogenic epitopes for the chimeric vaccine construct design. Proteins in the extracellular regions were prioritized for identifying B- and T-cell epitopes. ABCPred online resource was employed to predict B-cell epitopes from the prioritized protein sequences following a set threshold of >0.5. ABCPred identifies linear B-cell peptide sequences using Support Vector Machine (SVM) and artificial intelligence approaches (21). The Immune Epitope Database (IEDB) resource was utilized to identify T-cell epitopes. CD8+ helper T lymphocytes (HTL) are MHC-I-restricted epitopes that were determined using the Stabilized Scoring Method (SSM). MHC-II epitopes i.e., CD4+ cytotoxic T lymphocytes (CTL), were determined using the neural network-based scoring method (NetMHC 1.1). The human HLA reference alleles set was utilized with the IC_{50} <200 nM (22). Lead CTL, HTL, and linear B-cell epitopes were further prioritized based on immunogenic properties. The antigenic behavior of the prioritized epitopes was evaluated using the VaxiJen v2.0 web tool with a cut-off of 0.4 (23). The allergenicity of the epitopes was determined by AllerTOP 2.0 tool (24) and the toxicity was determined by the ToxinPred server (25).

2.6 Assessment of population coverage

Variations in the distribution and expression of HLA alleles among various ethnic groups and geographic regions around the world strongly impact the effectiveness of vaccine synthesis. Therefore, the global population coverage of the prioritized CTL and HTL epitopes and their respective HLA-binding alleles was determined using the IEDB population coverage tool (26). Conservation analysis is important to measure the degree of similarity between homologous peptides.

2.7 Multi-epitope chimeric vaccine designing

The top-ranked overlapped CTL, HTL, and linear B-cell epitopes of 9-20 mer were prioritized based on their antigenicity, allergenicity, and toxicity values to design chimeric vaccine models. The rationale behind the selection of overlapped epitopes was to induce both cell-mediated and humoral immune responses against the immunogenic antigen (27). Besides potential immunostimulatory adjuvants were used to induce enhanced immune responses and to initiate long-term innate immunity (28). Four different adjuvant sequences, i.e. HBHA protein, β-defensin, 50S ribosomal protein L7/L12, and HBHA conserved peptide sequence were used in designing the constructs. EAAAK linker (stiff spacer) was used to connect the adjuvant sequence to the N-terminus of the model construct (29). GGGS and HEYGAEALERG flexible linkers were used for effective epitope conjugation based on Solanki & Tiwari's (30) approach. PADRE sequences were also incorporated to enhance the vaccine construct stability and induce innate and adaptive immune responses. The linkers prevent junctional epitope development, enhance the expression and bioactivity of the vaccine construct, and stimulate robust immunogenic responses against the antigenic vaccine (30).

2.8 Physicochemical and immunological assessment of model vaccine constructs

The chimeric vaccine constructs were evaluated by following the physicochemical and immunological parameters. ExPASy ProtParam web tool was utilized to evaluate multiple physicochemical properties of the constructs (31). The solubility feature was calculated using the SOLpro web tool (32). The antigenicity, allergenicity, and toxicity evaluation of the vaccine constructs was conducted by Vaxijen v2.0 (23), AllerTOP2.0 (24), and ToxinPred2 (25) web servers, respectively. ANTIGENpro web tool evaluated the antigenic nature of the designed vaccine constructs. The tool uses 10-fold cross-validation of the antigenic peptides to calculate the protective capabilities of the peptide sequences based on known datasets (33).

2.9 Assessment of secondary and tertiary structures

PSIPRED v 4.0 (34) and SOPMA (35) tools were used to analyze and assess the secondary structure and composition quality aspects of the model vaccine constructs. These servers use a Position-Specific Scoring Matrix (PSSM) to predict transmembrane topologies, transmembrane helices, and peptide sequences with folds and domains. The tertiary structure of vaccine constructs was predicted using the Phyre2 web tool following 99% structure confidence parameter (36). The predicted 3D structures of the designed vaccine constructs were further refined using the GalaxyRefine tool. GalaxyRefine uses CASP10-based refinement approaches to achieve a relaxed protein structure based on repacking and molecular dynamic modeling techniques. This approach improves the quality of predicted protein models and enhance global and local structural features (37). After refinement, the 3D structures of the designed vaccines were validated by ERRAT, PROCHECK (38), and ProSA-web (39) servers. ProSA-

web server determines the overall quality of the vaccine structure by calculating the Z-score. The Z-score value beyond the threshold established for natural proteins indicates errors in the protein model (39). PROCHECK tool determines the geometry of the residues in protein structure and generates a Ramachandran plot to evaluate the stereochemical quality of the designed vaccine models.

2.10 Determination of discontinuous B-cell epitopes

Linear B-cell epitope determination is dependent upon the amino acid sequence of the designed vaccine. Nevertheless, certain epitopes are also conformational/discontinuous, relying on the 3D structure of the model vaccine rather than the linear sequence (40). The refined 3D structure of the model vaccine construct was subjected to the ElliPro web server to determine discontinuous B-cell epitopes. The server is based on residue clustering and Tornton's methods for discontinuous B-cell epitopes prediction and assigns PI (protrusion index) value to the predicted epitopes (40).

2.11 Molecular docking with host immune receptor

Molecular docking provides an insight into the binding interaction between the model vaccine constructs and the immune receptor proteins. The molecular docking study of the designed vaccine constructs with the human toll-like receptors 4 (TLR4) was conducted using the ClusPro resource. ClusPro is a robust and highly integrated protein-protein docking server that incorporates a hybrid docking algorithm based on experimental data of substrate binding site of protein and small-angle X-ray scattering to perform docking analyses to generate 10 models (41). The refined 3D structure of the vaccine construct (ligand) was docked against TLR4 (PDB:3FXI) receptor. The molecular interactions between the residues in the vaccine-TLR4 complex were demonstrated via the PDBsum (42).

2.12 Normal mode analysis

The normal mode analysis (NMA) was conducted for the finalized V1-TLR4 complex using the iMODS server (43) to demonstrate the internal dihedral coordinates and assess the cooperative functional motions of the peptide vaccine. The essential dynamic simulation program of iMODS was used to ensure the energy minimization, molecular stability, and atomic mobility of the prioritized vaccine construct in the docked complex. The server calculates the probable motions of the V1-TLR4 complex based on specialized parameters, including B-factors, eigenvalues, RMSD, deformability of the complex, covariance values, and elastic models (43).

2.13 Molecular dynamic simulation analyses

2.13.1 Desmond MD simulations

The MD simulations were performed to study the dynamics and stability of the vaccine-TLR4 docking complex using the Desmond program of Schrödinger suite 2023-1 (Schrödinger, LLC, New York, NY, USA) (44). The coordinate file and topology of the vaccine-receptor complex were generated using the Optimized Potentials for Liquid Simulation (OPLS4) force field in the initial step (45). The complex was further solvated in transferable intermolecular potential 3P (TIP3P) by adding a hydrated box with a boundary size of 10 Å (46), followed by counter ions (Na^+ and Cl^-) to neutralize the charges in the simulated system. Furthermore, energy minimization was carried out to acquire the desired threshold of ≥1000.0 kJ/mol/nm. NVT and NPT simulations were conducted for 1 ns, respectively, to generate a stable temperature and pressure environment. The temperature of the simulated system was equilibrated to 310 K and pressure was maintained at 1 atm. The Berendsen thermostat was used to regulate the temperature, and the Parinello-Rahman barostat was employed to equilibrate the pressure of the system. Finally, the hydrogen bonds were constrained using the LINCS technique, and the long-range electrostatic interactions were calculated using the Particle-Mesh Ewald summation scheme (47). The MD simulation was run with an isothermal and isobaric system for 200 ns.

2.13.2 Principal component analysis

The principal component analysis (PCA) was performed to detect the high amplitude primary movements and conformation changes from the MD trajectory. The principal components (PCs) are eigenvectors that identify the direction of motion, and the corresponding eigenvalues describe the degree of residual motion during the MD. Using the ProDy package, the covariance matrix was first measured by using the Cα coordinates, and then the covariance matrix was diagonalized to construct the eigenvalues and eigenvectors (PCs) (48). The mode vectors were visualized using VMD (Visual Molecular Dynamics) software to understand the relationship between the movements of the vaccine construct and the motions of TLR4 residues.

2.14 Computational immune simulations of model vaccine construct

The C-ImmSim web application was followed to perform computational immunological simulation of the top-prioritized designed vaccine model (49). The server computes cellular and humoral responses produced against the antigenic vaccine using PSSM and several machine-learning algorithms (50). The server uses antigenic peptide sequences and lymphocyte receptors to simulate the immunogenic responses. In this study, a standard clinical protocol of a four-week period between two doses was followed to conduct an immune simulation of the designed vaccine construct (51). The human host leukocyte antigens HLA-A*0101,

HLA-A*0201, HLA-B*0702, HLA-B*3901, HLA-DRB1*0101, and HLA-DRB1*0401 were selected for time periods of 1h, 84h, and 168h. Immune simulation was performed using default settings for 1000 steps (29).

2.15 Computational cloning assessment of optimized vaccine construct sequence

The reverse translation of the prioritized vaccine model was performed using the Java Codon Adaptation Tool (JCAT). Codons in the cDNA sequence of the construct were optimized to maximize the model vaccine's expression in the bacterial expression system (52). JCAT calculates codon adaptation index (CAI) and percentage CG content to assess the protein expression capability of the construct. The optimal CAI value is stated to be 0.8-1 and the GC content should range from 30 to 70% for promising transcriptional and translational efficacies of vaccine (29, 53). The *E. coli* strain K12 was chosen as the host organism for the expression of the model vaccine. *E. coli* strain K12 was selected because it is commonly used to clone human vaccines in mouse models against many pathogens and highly protective antibody production has been evident in experimental models using this strain (54). *E. coli* pET28(+) vector was retrieved from the Addgene server (55) for *in-silico* restriction cloning. The SnapGene program (https://www.snapgene.com/) was used to introduce the optimized construct sequence of the model vaccine in *E. coli* plasmid.

3 Results

3.1 Subtractive proteomics analysis

In the current study, we employed a subtractive proteomics strategy to determine parasite-specific vaccine candidate proteins to design multi-epitope vaccine constructs. A total of 8462 non-paralogous protein sequences of the *L. tropica* strain L590 were obtained from CD-Hit clustering recourse with a calling criterion of 0.8 (Supplementary File 1). Non-paralogous protein sequences were subjected to the DEG database and analysis identified a total of 1225 parasite essential proteins (Supplementary File 2). These proteins are responsible for the survival of the parasite and may be involved in pathogenesis. A total of 496 host non-homologous parasite-essential proteins were identified after screening against human and human gut proteomes (Supplementary File 3).

3.2 Subcellular localization and vaccine candidate selection

The parasite-essential proteins that were non-homologous to human and human gut proteomes, were prioritized for subcellular localization prediction. Analysis categorized proteins into cytoplasm, cytoplasmic membrane, extracellular, and cell wall localization (Table 1). Based on surface topology, five proteins i.e., LTRL590_220014100, LTRL590_090006100, LTRL590_100005200, LTRL590_180011200, and LTRL590_190013800 located in the extracellular region were prioritized and screened for B- and T-cell epitopes identification. LTRL590_220014100 is a conserved hypothetical protein predicted in the extracellular region of the parasite. LTRL590_090006100 is an RNA-binding 5-like protein that is associated with the post-transcriptional modulation of the parasite proteins and plays a major role in parasite survival and adaptation to the drastic environmental change from amastigotes into promastigotes (56). The LTRL590_100005200 is a putative helicase protein that is associated with cellular DNA repair pathways and maintains genome stability throughout the differentiation from amastigotes into promastigotes stages in the leishmania cycle, hence plays a crucial role in the survival of the pathogen (57). The putative FYVE zinc finger containing protein (LTRL590_190013800) plays a major role in the virulence of the *leishmania* parasite by mediating protein-protein interactions and membrane association (58). These proteins also bind to nucleic acids and play an essential role in transcription, translation, and other biological processes during the transition from amastigotes to promastigotes (59).

TABLE 1 Subcellular localization of host non-homologous essential proteins of *L. tropica*.

Subcellular localization	Number of proteins
Cytoplasm	264
Unknown	125
Cytoplasmic membrane	94
Extracellular	5
Cell wall	8

3.3 Lead B- and T-cell epitopes prediction

Five extracellular vaccine candidate proteins were prioritized to predict B and T-cell epitopes. These epitopes were ranked based on high antigenicity and low allergenicity, and toxicity values. Only two CTL and HTL epitopes of 9-15-mer were prioritized from each vaccine candidate protein based on an IC_{50} <200 nM using the IEDB analysis resource. Likewise, two linear B-cell epitopes of 20-mer were prioritized from each prioritized protein. The top-ranked antigenic, non-allergenic, and non-toxic linear B-cell, CTL, and HTL epitopes sharing overlap peptides were prioritized for engineering model chimeric vaccine constructs (Table 2). The prioritized MHC epitopes exhibited population coverage of 79% approximately. North America was found as the largest population coverage of MHC epitopes (84.33%). The tropical and sub-tropical regions exhibited the highest density of these epitopes (Figure 2). Therefore, the vaccine designed based on these epitopes will provide significant protection against leishmaniasis in these regions.

10.3389/fimmu.2023.1259612

TABLE 2 Prioritized B- and T-cell epitopes predicted by ABCPred and IEDB web servers.

Gene IDs	B-cell Epitopes	Score	MHC-I Epitopes	Alleles	IC_{50}	MHC-II Epitopes	Alleles	IC_{50}
LTRL590_220014100	MSLPNWSANRQSIGARAGPA	0.83	MSLPNWSANR	HLA-A*31:01 HLA-A*68:01 HLA-A*33:01	21.93	WGQLELDMSLPNWSA	HLA-DRB1*03:01 HLA-DRB3*01:01	171
	YTLDAAVCVPFGGSGADASR	0.87	YTLDAAVCV	HLA-A*02:06 HLA-A*02:01 HLA-A*68:02 HLA-A*02:06	17.17	HRYQYTLDAAVCVPF	HLA-DRB3*01:01 HLA-DRB3*02:02 HLA-DRB1*07:01	5.5
LTRL590_090006100	FFTPFGVTAGTESDLMASAL	0.87	SPAPAFFTPF	HLA-B*07:02 HLA-B*35:01 HLA-B*15:01	22.49	PAFFTPFGVTAGTES	HLA-DRB1*07:01	147.9
	RASSSNVTPINYSAHVVPSQ	0.85	STRASSSNV	HLA-A*30:01	7.35	GTFTESPGSTRASSS	HLA-DRB5*01:01	159.6
LTRL590_100005200	TLKRDERDDASGRDTRNLSF	0.88	FETLKRDERD	HLA-B*07:02	13.26	AVKRFYETLKRDERD	HLA-DRB5*01:01	38.2
	SRTQIPLRHAWALTIHKSQG	0.82	ASRTQIPLR	HLA-A*31:01 HLA-A*30:01 HLA-A*68:01 HLA-A*31:01	20.22	GIMVSSAASSASRTQ	HLA-DRB3*02:02	20.5
LTRL590_180011200	NGGAPSSTSVATVYASPTQA	0.88	TVYASPTQA	HLA-A*02:03 HLA-A*68:02	87.42	QVVYTASPTQAAGVM	HLA-DRB5*01:01	169.39
	PTPTQMLTPQANAAAAAAAV	0.86	TPAQPTPTQM	HLA-B*07:02 HLA-B*35:01	44.1	YTPDAFPTPTQMAAA	HLA-DRB1*07:01	181.26
LTRL590_190013800	YVAAPQDTGRASVGVEHRVI	0.88	KQDTSYVAA	HLA-A*02:06	19	SADYVAAAPGYSAHT	HLA-DRB5*01:01	118
	VVSNELAVSHKTCGREEAAT	0.88	VVSNELAVSH	HLA-A*33:01	195	VVSNELAVSRRRVLC	HLA-DRB4*01:01	33.18

The red color indicates the overlapping residues in the MHC-I, MHC-II, and B-cell epitopes.

3.4 Designing multi-epitope chimeric vaccine models

The overlapped lead CTL, HTL, and B-cell epitopes were used to engineer a highly immunogenic multi-epitope chimeric vaccine with the capability to elicit significant immune responses against *L. tropica*. Ten overlapping epitopes were selected and linked by GGGS and HEYGAEALERG linkers to design such a construct. Four different adjuvants were attached at the N-terminal of the multi-epitope peptide sequence using EAAAK linkers to design four different vaccine constructs. The vaccine construct-V1 was designed using HBHA adjuvant. Likewise, the V2, V3, and V4 constructs were designed using β-definsin, HBHA conserved protein, and ribosomal protein adjuvants respectively (Supplementary Data). PADRE peptides were inserted in the peptide sequence of the designed vaccine construct to overcome HLA-DR challenges

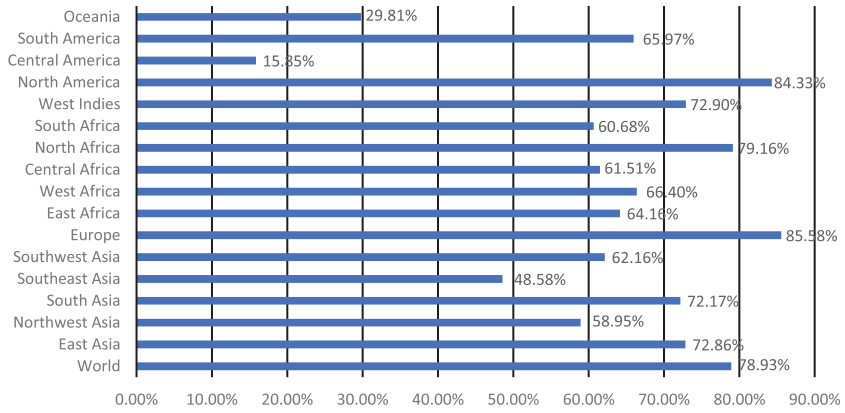

FIGURE 2
Population coverage of the prioritized MHC epitopes determined by IEDB analysis resource.

and enhance immune protection and HLA responses (60). The proposed vaccine constructs were designed to stimulate specific immune responses with reduced risk of antigen-induced anaphylaxis.

The immunological properties determined all four of the designed vaccine constructs to be highly antigenic, non-toxic, and non-allergenic in nature. VaxiJen v2.0 scores for all the constructs ranged from 0.96 to 1.15, which is above the set antigenic threshold. The estimated range of ANTIGENpro scores ranged from ~0.85 to ~0.95, indicating the highest antigenicity of the vaccine constructs. The estimated molecular weights of the designed vaccine constructs ranged from 36 to 48 kDa, indicating the ideal molecular weight for commercial production. The SOLpro values ranged from ~0.57 to ~0.60, suggesting high solubility of the vaccine constructs. The estimated GRAVY values were in the range of -0.068 and -0.278, suggesting the hydrophilic nature of the model constructs. The theoretical pI scores ranged from 5.59 to 9.63, the aliphatic index ranged from 62.79 to 74.27, and the instability index values ranged from 32.29 to 43.00. These results indicate the thermostability of the model vaccine constructs at different temperature ranges. All of the model vaccine designs were non-allergenic, non-toxic, and highly antigenic due to their physicochemical and immunological features. The stringent threshold of physicochemical and immunological characteristics predicted that the proposed constructs depict thermostability and substantial abilities to stimulate strong immunogenic responses against leishmaniasis (Tables 3 and 4).

3.5 Secondary and tertiary structures prediction, refinement, and validation

The secondary structure prediction analysis unraveled that the designed vaccine constructs (V1-V4) comprise ~32% to 52% α-helices, ~5% to 10% β-stands, ~29% to 43% random coils, and ~11% to 18% extended strains. The tertiary structure prediction of all four vaccine constructs was performed using a homology-based strategy. The modeled structures were further refined to generate high-quality 3D structure models. Ramachandran plot analysis depicted that ~91 to 99% of residues of the refined vaccine structure models occurred in the core region of the plot. ERRAT values were calculated to be in the range of ~97 to 100 and the Z-scores for the proposed vaccine models were estimated between -3 to -7 (Table 5). These results suggest that the designed vaccine construct models were of high quality with significant 3D structural stability. The secondary and tertiary structures of the top prioritized model vaccine-V1 have been shown in Figure 3.

3.6 Discontinuous B-cell epitopes prediction

Explicit interactions occur between B-cells and the epitopes at a 3D level in their folded state. Therefore, discontinuous/conformational epitopes with various residues were determined

TABLE 3 Physicochemical properties, % GC content, and CAI values of the model vaccine constructs calculated by ProtParam and JCAT tools.

Vaccine construct	Adjuvants	Number of Amino Acids	Molecular Weight (Daltons)	Theoretical pI	Aliphatic index	Grand average of hydropathicity (GRAVY)	Instability index	GC content	CAI
V1	HBHA	476	48kDa	5.81	71.83	-0.278	39.59	50%	1.0
V2	β-defensin	362	36kDa	9.63	62.79	-0.235	38.31	50.73%	1.0
V3	HBHA conserved	567	47kDa	5.59	73.81	-0.253	43.00	49.73%	1.0
V4	Ribosomal protein	457	44kDa	5.91	74.27	-0.068	32.29	48.83%	1.0

10.3389/fimmu.2023.1259612

TABLE 4 Immunological properties and docking scores of the designed vaccine constructs.

Vaccine construct	Allergenicity	Antigenicity (Vaxijen 2.0 scores)	ANTIGENpro Scores	SOLpro scores	Docking score against TLR4 (kcal/mol)
V1	Non-Allergen	0.9952	0.886112	0.576670	-886.7
V2	Non-Allergen	1.1411	0.948980	0.599276	-869.1
V3	Non-Allergen	1.0045	0.844777	0.607072	-882.3
V4	Non-Allergen	0.9685	0.913701	0.570929	-592.9

TABLE 5 Secondary and tertiary structures prediction and validation of the designed vaccine constructs.

Vaccine Constructs	Alpha Helices	Extended strand	Beta turns	Random coil	ERRAT	PROCHECK Ramachandran core region	ProSA-Web Z-score
V1	51.89%	11.13%	5.67%	31.30%	97.9592	94.0%	-3.95
V2	32.04%	17.13%	8.56%	42.47%	100	86.8%	-4.61
V3	53.10%	11.35%	5.78%	29.76%	98.2759	91.6%	-3.33
V4	43.62%	14.32%	9.17%	32.89%	100	98.3%	-7.25

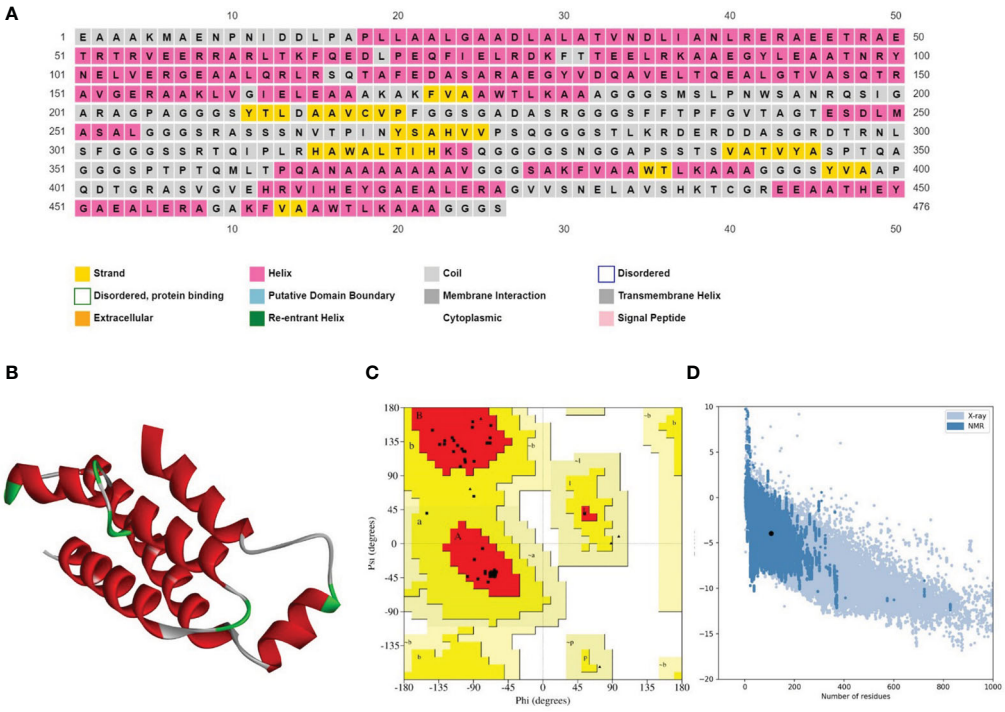

FIGURE 3
(A) Secondary structure prediction of the prioritized vaccine construct-V1 acquired from the PSIPRED server revealed that the majority of the structure comprises of α-helices and coils. **(B)** Refined 3D structure of the prioritized vaccine construct-V1. **(C)** Ramachandran plot of the prioritized vaccine construct-V1 showing model accuracy **(D)** ProSA-web results of the prioritized vaccine construct-V1 show a Z-score of -3.95, representing stable tertiary structure with minimum errors.

TABLE 6 Discontinuous B-cell epitopes predicted by ElliPro web tool.

No.	Residues	Number of residues	Score
1	A:F80, A:T81, A:T82, A:E83, A:E84, A:L85	6	0.855
2	A:G107, A:E108, A:A109, A:A110, A:Q112, A:R113, A:L114, A:R115, A:S116, A:Q117, A:T118, A:A119, A:F120, A:E121	14	0.796
3	A:Q66, A:D68, A:P70, A:E71, A:I74, A:E75, A:L76, A:R77, A:D78, A:K79	10	0.644
4	A:E42, A:E45, A:E46, A:T47, A:R48, A:A49, A:E50, A:T51	8	0.618

from the 3D structure of the finalized vaccine construct. The ElliPro web tool identified 4 conformational B-cell epitopes at a threshold of 0.5 and scores varied from 0.618 to 0.855. The size of the epitopes ranged from 6 to 14 amino acid residues (Table 6 and Figure 4).

3.7 Vaccine-TLR4 docking analysis

Molecular interaction between the vaccine construct and human immune receptor is crucial for understanding the antigenic potential of the designed vaccine construct to elicit immunogenic responses. TLR4 immune receptor is involved in recognizing pathogenic proteins, which in turn triggers the generation of inflammatory cytokines. Numerous studies have reported that TLR4 is essential for generating innate immune responses against an array of infections (61, 62). The molecular docking studies were carried out to evaluate the molecular interactions between vaccine constructs. All four vaccine constructs were docked against the human TLR4 receptor. The vaccine construct-V1 in complex with TLR4 exhibited the lowest binding energy of -886.7 kcal/mol. (Figure 5A and Table 5). The lowest binding energy measured the highest binding affinity between the vaccine construct-V1 and the TLR4 receptor. A feasible molecular interaction was found among vaccine construct-V1 and TLR4 receptor residues (Figure 5B). A total of two salt bridges, ten hydrogen-bond interactions (Figure 5C), and 151 non-bonding interactions were observed between the construct-V1-TLR4 complex chains. These results signified the ability of the vaccine construct to stably bind with immune receptors and induce an immunological response in the human immune system against leishmaniasis.

3.8 Normal mode analysis

The normal mode analysis (NMA) was conducted to establish the molecular stability and functional motions of the construct-V1-TLR4 complex (Figure 6). The deformability graph showed peak points that represent the main chain residues deformed regions in the V1-TLR4 complex. The high deformability regions can be used to determine the 'hinges/linkers' in the main chain (Figure 6A). The experimental B-factor plot demonstrates the association among the NMA mobility and V1-TLR4 complex, representing the average RMSD values of the docked complex (Figure 6B). The computed eigenvalue of the V1-TLR4 complex was 6.748725e-05 which reflects the motion stiffness linked to each normal mode (Figure 6C). Each normal mode of the complex is represented by an individual (purple) and cumulative (green) variance in the variance bar. Variance and eigenvalue were negatively correlated (Figure 6D). Additionally, the interacting motions between the two molecules in a complex are represented by a covariance map. In the current study, interrelated motions among different pairs of

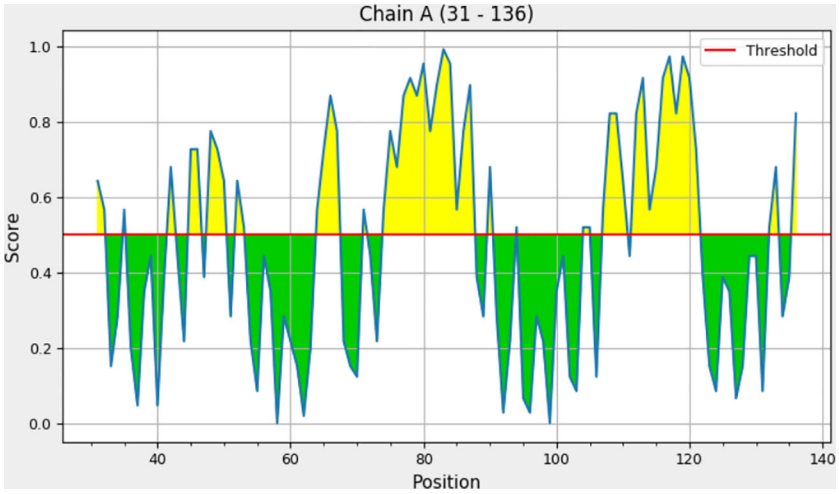

FIGURE 4
ElliPro residue score chart for each discontinuous B-cell epitope with a score above 0.6.

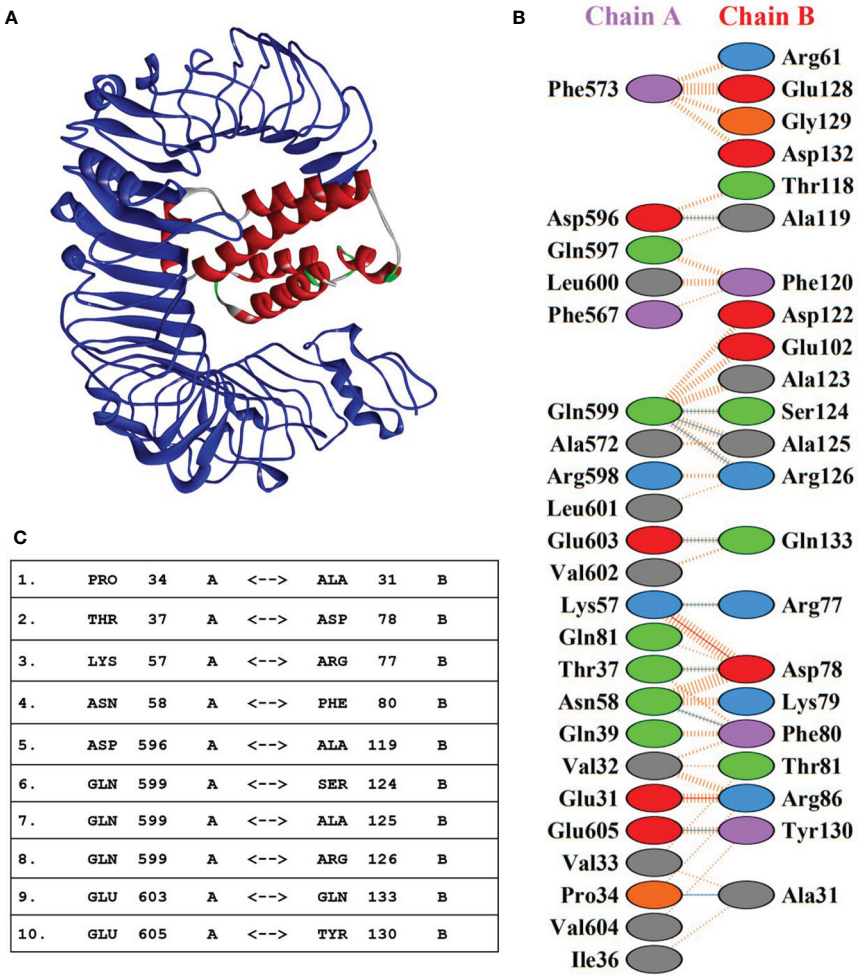

C

1.	PRO	34	A	<-->	ALA	31	B
2.	THR	37	A	<-->	ASP	78	B
3.	LYS	57	A	<-->	ARG	77	B
4.	ASN	58	A	<-->	PHE	80	B
5.	ASP	596	A	<-->	ALA	119	B
6.	GLN	599	A	<-->	SER	124	B
7.	GLN	599	A	<-->	ALA	125	B
8.	GLN	599	A	<-->	ARG	126	B
9.	GLU	603	A	<-->	GLN	133	B
10.	GLU	605	A	<-->	TYR	130	B

FIGURE 5
(A) 3D representation of the docking complex of vaccine construct V1 (red) with human TLR4 receptor (blue). **(B)** Molecular interactions between chain-A of TLR4 receptor molecule and chain-B of vaccine construct-V1. **(C)** Hydrogen-bond interaction between chain-A of TLR4 receptor molecule and chain-B of vaccine construct-V1.

residues were specified by correlated (red), uncorrelated (white), and anti-correlated (blue) atomic motions in the V1-TLR4 complex (Figure 6E). The specialized electric network map was also generated which represents pair of atoms connected by spring in the V1-TLR4 complex. The assembly between corresponding atoms of larger molecules and their stiffness are represented by colored dots, where the darker greys represent rigid springs (Figure 6F). Eventually, the NMA analysis anticipated stable interaction between the TLR4 and the prioritized vaccine construct-V1.

3.9 Molecular dynamic simulation analyses

3.9.1 Dynamics stability and residual flexibility of modeled vaccine–TLR4 complex

The root mean square deviation (RMSD) in the bound and unbound state of the vaccine construct and TLR4 receptor were calculated and presented as a graph based on the Cα atoms of the protein to explain the dynamic behavior and conformational stability from initial structure conformation to its final state (Figure 7A). Minor deviations faced by a system in the RMSD curved indicate a stable complex formation and vice versa; for the bound state, i.e., vaccine construct in complex with TLR4 receptor. The average RMSD of 4.03 Å depicts no significant fluctuation after convergence for the entire period of simulation except minor fluctuations at 20 and 125 ns. Afterward, the system was fully converged with a standard deviation of 0.54. Furthermore, the individual chains of the TLR4 receptor and vaccine construct revealed the mean RMSD of 2.57 Å and 5.49 Å (Figures 7B, C), with a standard deviation of 0.38 and 0.70, respectively. The highly deviated residues based on Cα is represented in the right panel of the figure which shows that only a few residues of the vaccine fluctuated to reorient itself. This is more probably due to the strain energy upon binding with TLR4. The rest of the vaccine remained stable and predicted to interact strongly with the receptor throughout the production run. In order to further comprehend the stability of the complex formation we carried out the residual flexibility analysis which indicates the TLR4 receptor has a lower flexibility value at the binding interface i.e., Pro34, Thr37, Lys57, Asn58, Asp596, and Gln599 (Figure 7D) which is congruent to our

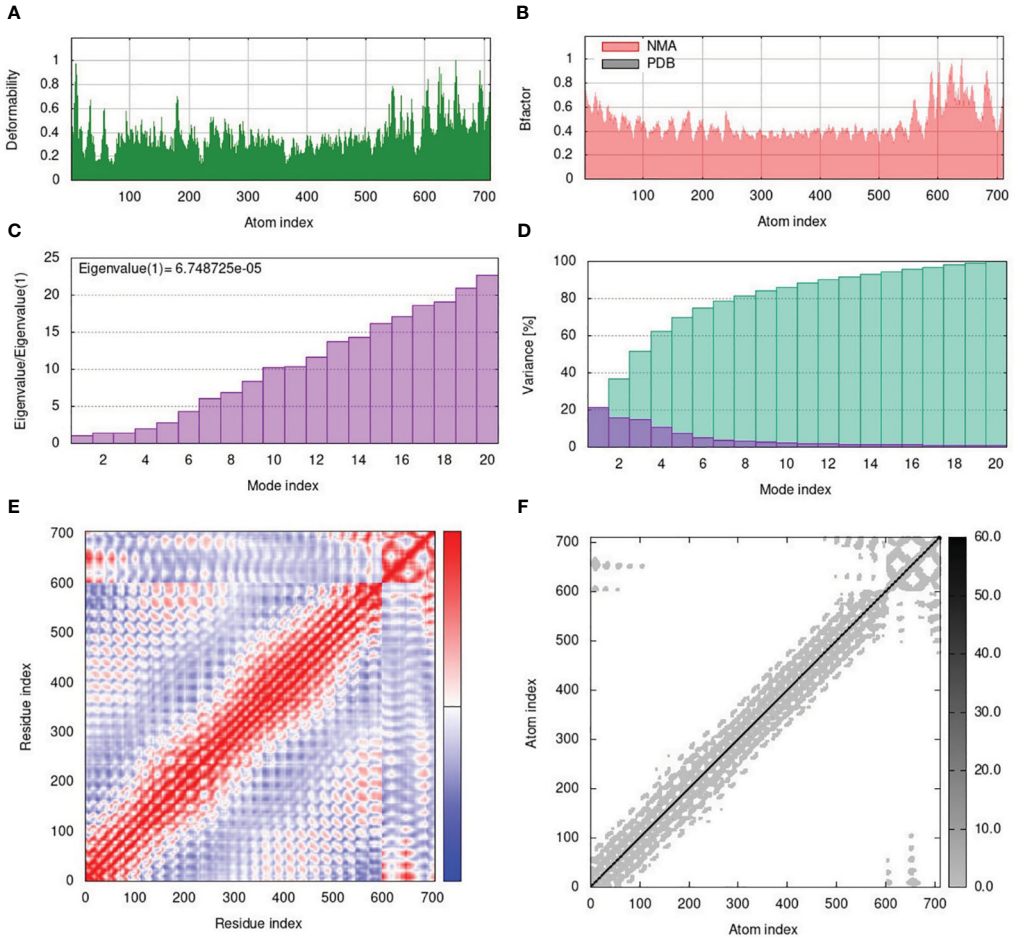

FIGURE 6
(A) The main-chain deformability of the V1-TLR4 complex deformed at each of its residues showing the location of the 'hinges/linkers' in the peptide chain. **(B)** The B-factor represents the associated PDB field and NMA mobility in the V1-TLR4 complex. **(C)** The eigenvalue specifies the motion stiffness linked to each normal mode. **(D)** The variance map is associated with individual (red) and cumulative (green) variances. **(E)** The covariance graph represents correlated (red), uncorrelated (white), or anti-correlated (blue) mobility of the pairs of residues in the V1-TLR4 complex. **(F)** The elastic network model describes the pairs of atoms connected by springs where the darker grey dots indicate the stiffness of the springs.

previous analysis. Overall, these findings demonstrated that vaccine construct in complex with TLR4 receptor showed significant dynamic stability for the entire 200 ns of the simulation period.

3.9.2 Principal component analysis

PCA was used to identify the predominant movements in TLR4 and vaccine construct-V1, and the majority of the combined dominating motions were represented by the first five eigenvectors. The first five eigenvectors for each system had significant variations, whereas subsequent eigenvectors displayed minor changes in amplitude, suggesting that the first five eigenvectors primarily represented the dynamic structural information. Herein the vaccine construct-V1 and TLR4's first two eigenvectors i.e., PC1 and PC2, were projected against one another to display potential attributed movements. The continuous color representation from deep blue to yellow shows the periodic transition between conformations. Each dot depicts the conformation of each frame; in the case of the TLR receptor, a constant frame overlapping was observed (Figures 8A, C). In contrast, the vaccine construct initially underwent fluctuation at the start of the simulation due to the strain energy; however, it did not exhibit any significant internal movements after 40ns, which further supported the RMSD results (Figures 8B, D).

3.10 Immune simulations

The immune simulation results showed a significant increase in primary and secondary immune responses against the top-ranked proposed vaccine construct-V1 (Figure 9). High levels of IgG1 + IgG2, IgM, and IgM + IgG immunoglobin antibodies were observed after the vaccine administration, representing proliferation of immune responses (Figure 9A). Increase in the B-cell population was evident after repeated exposure of the antigenic vaccine, resulting in the development of humoral immune memory (Figures 9B, C). The population of cytotoxic and helper T cells increased with a substantial decrease in the antigen population during secondary and tertiary immune responses (Figures 9D, E). This indicates the enhanced adaptive immunity capability of the proposed vaccine model (63, 64). Moreover, the development of

10.3389/fimmu.2023.1259612

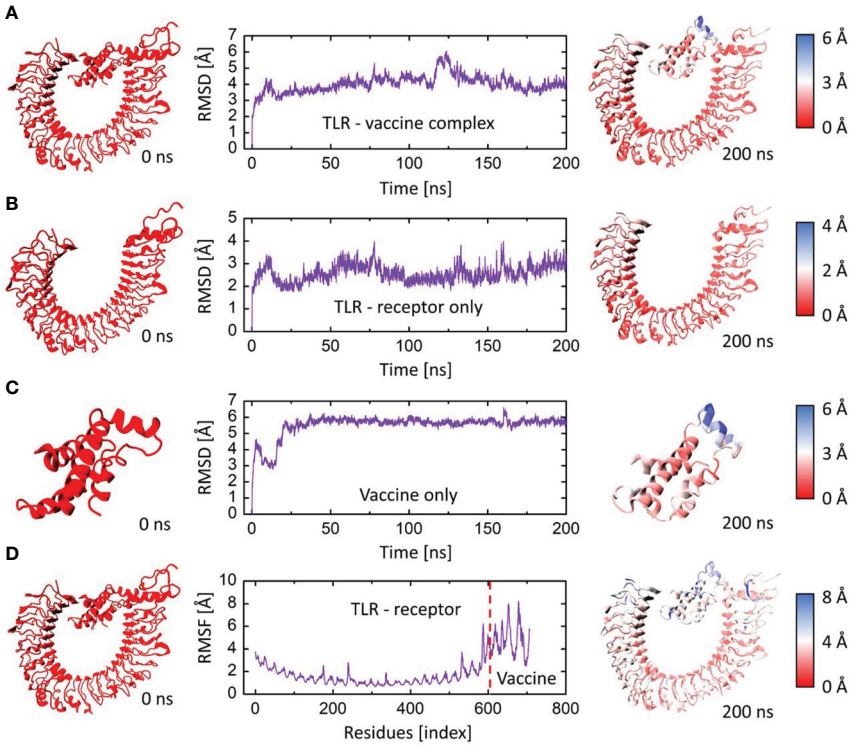

FIGURE 7
The RMSD and RMSF plots for TLR4 and vaccine construct complex. **(A)** RMSD plot of the vaccine-TLR4 complex. **(B)** RMSD plot of TLR4 receptor. **(C)** RMSD plot of vaccine construct. **(D)** RMSF plots for the vaccine-TLR4 complex. The left panel indicates the initial structure of the moieties, and the rightmost panel indicates the final conformation of the moieties. The colors are based on the Cα deviation based on the scales given for each representation.

natural killer cells, dendritic cells, and macrophages was also predicted to sustain growth after each immunization (Figures 9F–H). Vaccine dosages are commonly reported to stimulate the release of a variety of cytokines, including IFN-gamma, IL-23 (interleukin-23), IL-10, and IFN-beta, that eventually promote an immune response against infection (65, 66). In the case of the proposed construct-IV, significantly elevated levels of cytokines and interleukins, including IFN-γ and TGF-B, were predicted after continuous antigen exposure during immunization periods, while the other cytokines present lower concentration detection (Figure 9I). The Simpson's Index (D) was measured normal, indicating that vaccine-V1 has an analytically broader impact (67). These immune simulation predictions suggest that the prioritized vaccine-V1 has the potential to activate T and B cells to produce antibodies, leading to the development of long-lasting memory cells after repeated antigen exposure. The immune simulation prediction suggested that the vaccine construct V1 holds the potential to induce strong innate and adaptive immune responses in the human immune system against leishmaniasis.

3.11 Codon optimization and *in silico* restriction cloning

The expression potential of the proposed constructs was examined. The JCAT results for the optimized cDNA predicted that all the proposed vaccine constructs exhibited CIA values of 1.0 and GC content of 48-51%, which are within the optimal range of favorable expression of vaccine constructs in the *E. coli* K12 vector (Table 4) (68). The optimized gene sequence of the prioritized vaccine construct was predicted to successfully clone in the commonly used pET128 (+) plasmid with a total length of 6323 bp (Figure 10).

4 Discussion

L. tropica is one of the major causes of leishmaniasis, affecting millions of individuals worldwide. The World Health Organization (WHO) has listed leishmaniasis as one of the most neglected tropical diseases (6). Therefore, the development of novel treatment strategies is critical for providing protection against leishmaniasis. The availability of a potent vaccine against leishmaniasis is the most efficient and cost-effective approach to reduce mortality and morbidity. Advances in next-generation sequencing technology and the availability of massive genomic and proteomic data in public databases have led to the development of novel approaches, including immunoinformatics and reverse vaccinology, for identifying novel vaccine candidates against life-threatening pathogens in a cost- and time-effective manner (69, 70). Multiple preclinical trials were conducted to evaluate numerous vaccine candidates against leishmaniasis;

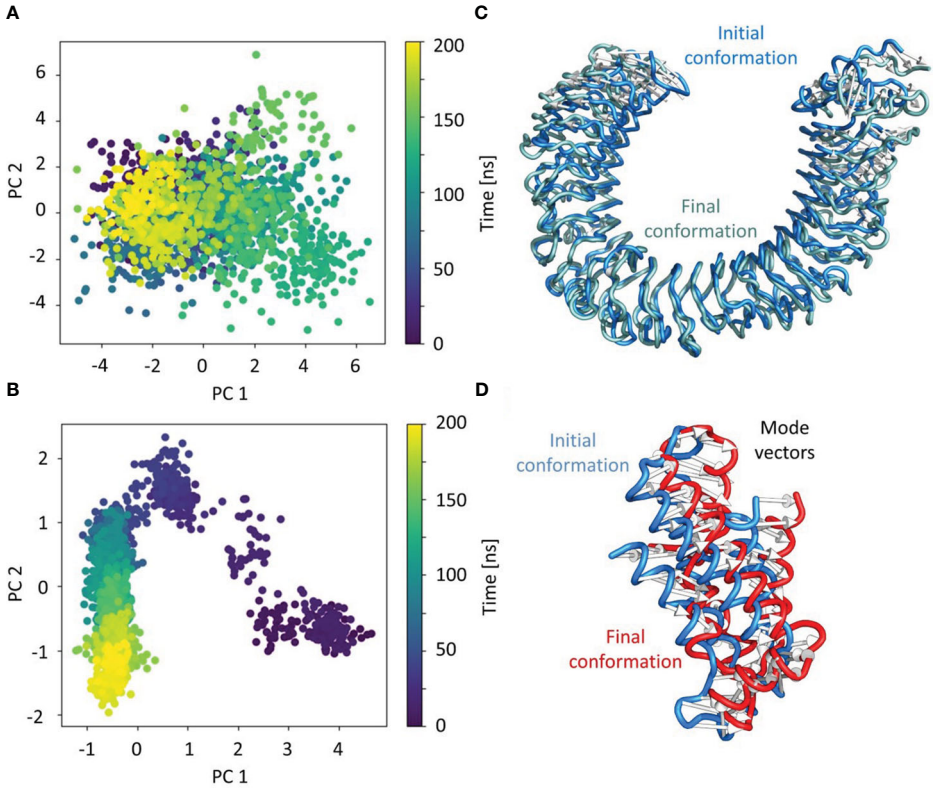

FIGURE 8
Individual principal component analysis of the conformational shifts in **(A)** TLR4 receptor, **(B)** the movements of the first principal component of the receptor from initial (cyan) to final (grey), **(C)** the vaccine construct, and **(D)** the movements of the first principal component of the vaccine construct from initial (cyan) to final (grey). The PC's color represents the progression through the trajectory from 0 ns (dark blue) to 200 ns (yellow).

however, a few have advanced to the clinical trial stage (71). Currently, no commercial vaccine is available against leishmaniasis. Previous studies targeted *L. major* and *L. infantum* to map potential epitopes against these pathogens (72). Likewise, a multi-epitope vaccine previously proposed against *L. donovani*, which also causes leishmaniasis (73). The present study aimed to design a next-generation multi-epitope chimeric vaccine against leishmaniasis that is capable of eliciting the human immune system and generating innate and adaptive immunity against *L. trotpica*-mediated infection.

In this study, we prioritized five extracellular *L. tropica* proteins as vaccine candidates. These proteins were non-homologous to human and human gut proteomes, as well as reported to be essential for the survival of the parasite. These proteins are predicted to be located in the extracellular regions and possibly be the first molecules to interact with the host cells; hence, making them ideal vaccine candidates to target (74). Stringent criteria were followed to identify CTL, HTL, and linear B-cell epitopes. B-cells induce humoral immune responses that neutralize pathogenic reagents and establish a memory to defend against future exposures (75). T cells, i.e., CTLs and HTLs, trigger cellular immune responses that prevent the spread of disease by eradicating infected cells or by secreting anti-microbial cytokines that provide long-lasting immunity for decades (76). B- and T-cell epitopes were further prioritized based on antigenicity, non-allergenic, and non-toxic parameters. The selected epitopes covered approximately 80% of the global population. Overlapping lead MHC-I, MHC-II, and B-cell epitopes in combination with specific linker and adjuvant sequences were used to design multi-epitope-based chimeric vaccine constructs. Similar *in-silico* strategies have been used to design vaccine constructs against multiple pathogens, including *Acinetobacter baumannii, Salmonella Typhimurium, Trypanosoma vivax*, COVID-19, Ebola virus, and Marburg, which have been validated experimentally (77–81). The designed vaccine models in this study are predicted to exhibit high antigenicity as well as low allergenicity and toxicity. The predicted physicochemical properties proposed that the vaccine constructs were highly stable with enhanced hydrophilicity, suggesting their ability to induce strong immunogenic responses in the human immune system. Thermodynamic stability, small molecular weight, and solubility predicted that the vaccine construct could easily be produced and administered in the host.

The 3D structural information is crucial to examine the activity of the vaccine by understanding the biomolecular interactions of the proposed vaccine to human immune cell receptor molecules. The tertiary structural prediction and validation of the proposed vaccines were carried out using multiple computational tools. The proposed vaccine constructs were significantly improved and displayed desirable characteristics in terms of quality and stability

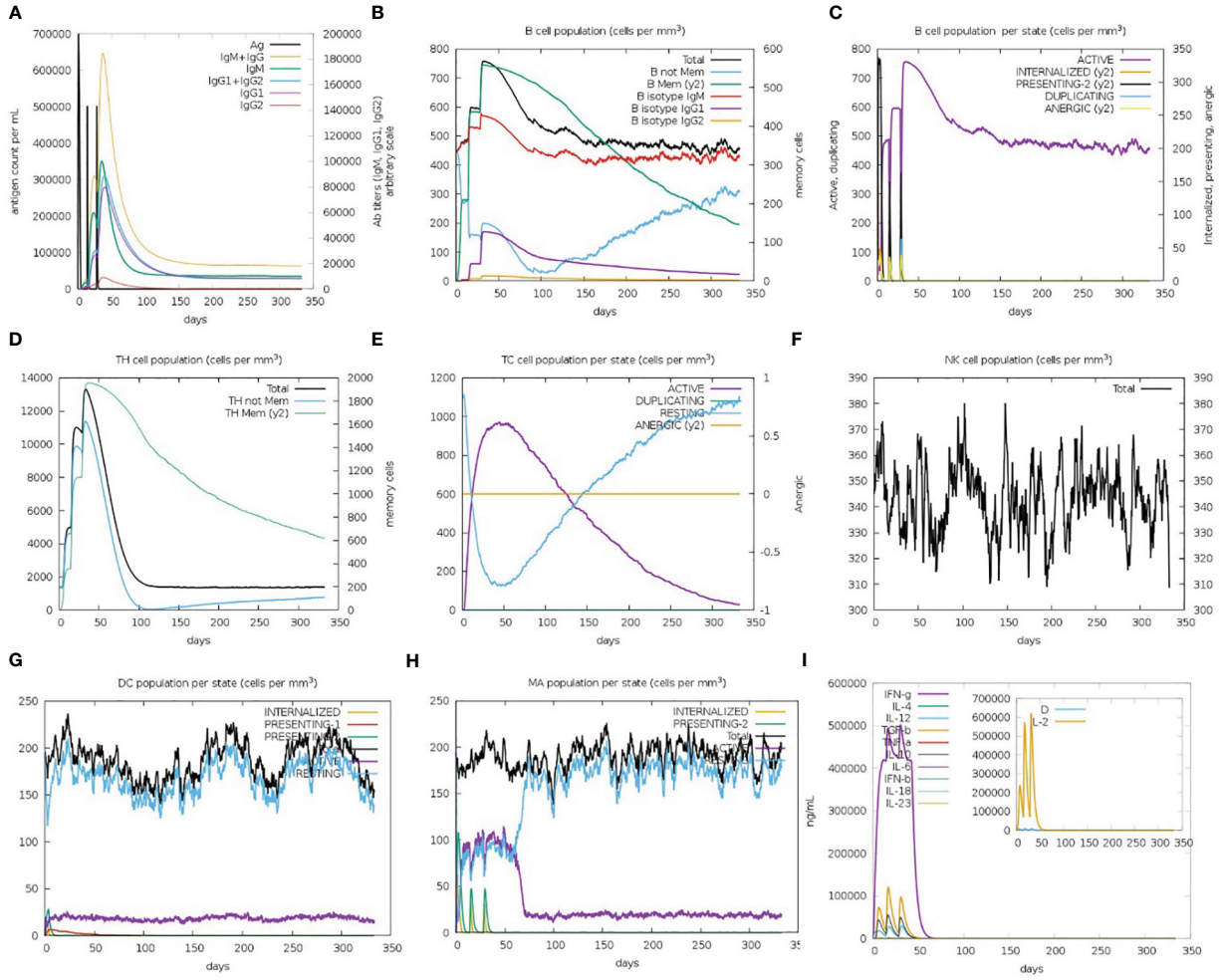

FIGURE 9
(A) Immunoglobin antibodies production after vaccination, representing proliferation of immune responses against the antigen **(B, C)** B-cell population increased after vaccine administration and development of memory B-cells. **(D, E)** The population of helper and cytotoxic T cell increase with a decrease in the antigen population and development of memory cell. **(F–H)** Development of natural killer cells, dendritic cells, and macrophages. **(I)** High levels of cytokines and interleukins after continuous antigen exposure.

as predicted by Ramachandran plot values and Z-scores. Previous studies reported that human TLR receptors have been associated with the identification of pathogenic peptides and are responsible for the stimulation of immune responses against specific pathogens (82). Therefore, the molecular docking analysis of *L. tropica* vaccines was carried out against human TLR4 receptors. The docking results determined strong binding interactions between vaccine-TLR4 complexes. Vaccine construct-V1 showed the lowest binding energy with the human TLR4 receptor. The thermodynamic stability of the V1-TLR4 complex was verified by binding affinity, normal mode dynamics, and immune simulations analyses (83–86). Immunogenic responses of TLR4 have been reported previously to inhibit parasite load and reduce inflammation in CL (82). Immune simulations indicated regular and effective immune responses. Stronger immune responses were triggered as a result of repeated exposure to the antigenic vaccine construct-V1. Helper T cells were stimulated and memory B and T cells were found to develop. Strong Ig and Th-cell production enhanced the humoral immune response. A similar study reported the same immune patterns for various pathogens (78, 79, 87). The C-ImmSim application prediction has been validated experimentally in recent studies that reported more or less the same immunization pattern against viral antigens as predicted by the resource (88, 89). The results suggested that the prioritized vaccine construct-V1 holds significant potential to activate human TLR receptors and trigger both humoral and cell-mediated immune responses against leishmaniasis. The computational restriction cloning of the vaccine cDNA sequence in an *E. coli* plasmid ensured the expression capability of the vaccine construct-IV in the bacterial expression system. All the analyses pursued lay a framework for the development of an effective anti-leishmania vaccine capable of eliciting significant immunological responses in the human host immune system.

The current study presents a multi-epitope chimeric vaccine design utilizing the *L. tropica* protein components, which is one way to deal with antigenic complexities. However, the current study holds some limitations. Immunoinformatics-based vaccine construction depends heavily on prediction methods. The degree

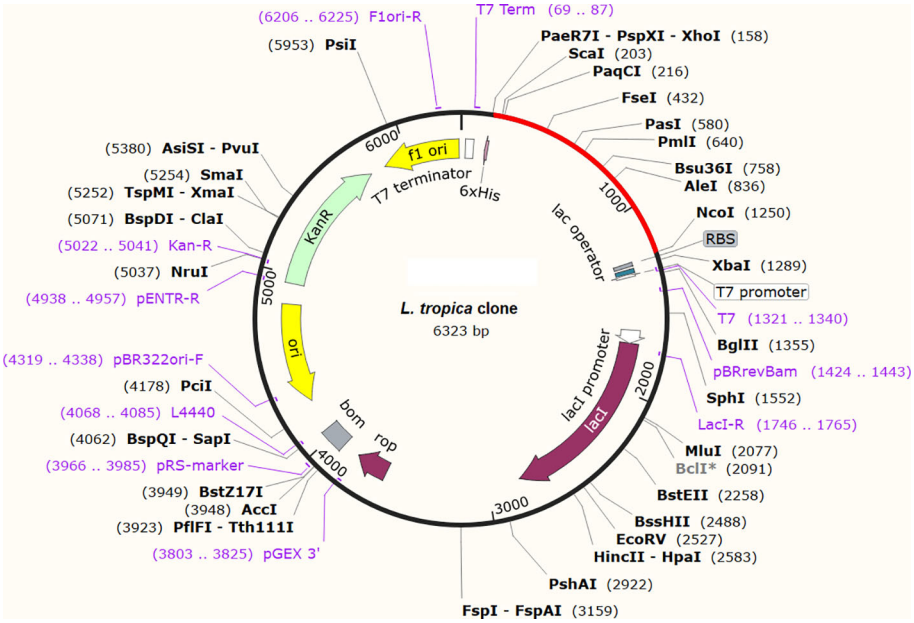

FIGURE 10
In-silico restriction cloning of the optimized gene sequence of the finalized vaccine construct in *E. coli* vector. The red color indicates the sequence of the vaccine and the black color indicates the sequence of the plasmid.

of protection against *L. tropica* infection is unclear, and the accuracy of these prediction approaches may be limited. Standard benchmarking, restricted prediction methodologies, and a lack of accurate datasets for diverse computational studies are only a few of the difficulties associated with immunoinformatics-based methods. Although immunoinformatics predictions have led to some positive case reports in recent years (90–92), the findings of this study still need to be investigated through *in vitro* and *in vivo* bioassays to confirm the safety and effectiveness of the proposed vaccine against leishmaniasis.

5 Conclusion

The current work employs subtractive proteomics and reverse vaccinology strategies to generate a novel multi-epitope chimeric vaccine construct against *L. tropica*. Extracellular proteins were used to identify B- and T-cell epitopes. Lead overlapping B- and T-cell epitopes were prioritized based on antigenicity, allergenicity, and toxicity characteristics to create a unique multi-epitope vaccine construct. The immunological features predicted the prioritized vaccine models to be non-allergenic, non-toxic, and highly antigenic. The physiochemical features predicted structure stability, and high solubility of the proposed vaccine models. Molecular docking, normal mode analysis, and molecular dynamic simulations established the stability and strong binding interactions of the top-ranked vaccine construct with human immune receptors. Immunological simulation revealed that the proposed vaccine design is capable of eliciting cell-mediated and humoral immune responses in the host immune system. The findings of this study needs to be validated experimentally.

Data availability statement

The original contributions presented in the study are included in the article/Supplementary Material. Further inquiries can be directed to the corresponding authors.

Author contributions

SA: Formal Analysis, Investigation, Methodology, Writing – original draft, Writing – review & editing. AA: Data curation, Formal Analysis, Writing – original draft, Writing – review & editing. AAK: Methodology, Writing – review & editing. AM: Writing – review & editing. AS: Writing – review & editing. SA: Formal Analysis, Writing – review & editing. CL: Writing – review & editing. ZR: Funding acquisition, Supervision, Writing – review & editing. AK: Data curation, Formal Analysis, Writing – review & editing. SK: Writing – review & editing, Supervision, Writing – original draft.

Funding

The authors declare financial support was received for the research, authorship, and/or publication of this article. This work was funded by the Researchers Supporting Project Number (RSP2023R339) at King Saud University, Riyadh 11451, Saudi Arabia, and the National Natural Science Foundation of China grant Nos. 31902287.

Acknowledgments

The study was approved by the Faculty of Environmental and Life Sciences, Beijing University of Technology, Beijing 100124, China, and the National Natural Science Foundation of China grant Nos. 31902287.

Conflict of interest

The authors declare that the research was conducted in the absence of any commercial or financial relationships that could be construed as a potential conflict of interest.

Publisher's note

All claims expressed in this article are solely those of the authors and do not necessarily represent those of their affiliated organizations, or those of the publisher, the editors and the reviewers. Any product that may be evaluated in this article, or claim that may be made by its manufacturer, is not guaranteed or endorsed by the publisher.

Supplementary material

The Supplementary Material for this article can be found online at: https://www.frontiersin.org/articles/10.3389/fimmu.2023.1259612/full#supplementary-material

SUPPLEMENTARY FILE 1
multi-fasta file containing non-paralogous proteins from *L. tropica*;

SUPPLEMENTARY FILE 2
multi-fasta file of parasite essential proteins;

SUPPLEMENTARY FILE 3
parasite essential proteins that are non-homologous to human and human gut microbiota.

SUPPLEMENTARY DATA SHEET
all four designed vaccine constructs.

References

1. Rostamian M, Niknam HM. Leishmania tropica: What we know from its experimental models. *JAiP* (2019) 104:1–38. doi: 10.1016/bs.apar.2018.11.001

2. Khan A, Sajid R, Gul S, Hussain A, Zehri MT, Naz S, et al. Epidemiological and pathological characteristics of Cutaneous Leishmaniasis from Baluchistan Province of Pakistan. *Parasitology* (2021) 148(5):591–7. doi: 10.1017/S0031182020002413

3. Salloum T, Moussa R, Rahy R, Al Deek J, Khalifeh I, El Hajj R, et al. Expanded genome-wide comparisons give novel insights into population structure and genetic heterogeneity of Leishmania tropica complex. *PloS Negl Trop Dis* (2020) 14(9): e0008684. doi: 10.1371/journal.pntd.0008684

4. McGwire BS, Satoskar AR. Leishmaniasis: clinical syndromes and treatment. *QJM: Int J Med* (2014) 107(1):7–14. doi: 10.1093/qjmed/hct116

5. Mann S, Frasca K, Scherrer S, Henao-Martínez AF, Newman S, Ramanan P, et al. A review of leishmaniasis: current knowledge and future directions. *Curr Trop Med Rep* (2021) 8(2):121–32. doi: 10.1007/s40475-021-00232-7

6. Aiman S, Alzahrani AK, Ali F, Abida, Imran M, Kamal M, et al. Comparative Proteomics and Genome-Wide Druggability Analyses Prioritized Promising Therapeutic Targets against Drug-Resistant Leishmania tropica. *Microorganisms* (2023) 11:228. doi: 10.3390/microorganisms11010228

7. Abdellahi L, Iraji F, Mahmoudabadi A, Hejazi SH. Vaccination in leishmaniasis: A review article. *Iranian Biomed J* (2022) 26(1):1–35. doi: 10.52547/ibj.26.1.35

8. Moafi M, Rezvan H, Sherkat R, Taleban R. Leishmania vaccines entered in clinical trials: A review of literature. *Int J Prev Med* (2019) 10:95. doi: 10.4103/ijpvm.IJPVM_116_18

9. Seyed N, Taheri T, Rafati S. Post-genomics and vaccine improvement for leishmania. *Front Microbiol* (2016) 7:467. doi: 10.3389/fmicb.2016.00467

10. Dikhit MR, Kumar A, Das S, Dehury B, Rout AK, Jamal F, et al. Identification of Potential MHC Class-II-Restricted Epitopes Derived from Leishmania donovani Antigens by Reverse Vaccinology and Evaluation of Their CD4+ T-Cell Responsiveness against Visceral Leishmaniasis. *Front Immunol* (2017) 8:1763. doi: 10.3389/fimmu.2017.01763

11. Rinaudo CD, Telford JL, Rappuoli R, Seib KL. Vaccinology in the genome era. *J Clin Invest* (2009) 119(9):2515–25. doi: 10.1172/JCI38330

12. Gheorghe G, Ilie M, Bungau S, Stoian AMP, Bacalbasa N, Diaconu CC. Is there a relationship between COVID-19 and hyponatremia? *Medicina (Kaunas Lithuania)* (2021) 57(1):55. doi: 10.3390/medicina57010055

13. Warren WC, Akopyants NS, Dobson DE, Hertz-Fowler C, Lye LF, Myler PJ, et al. Genome assemblies across the diverse evolutionary spectrum of leishmania protozoan parasites. *Microbiol Resour Announc* (2021) 10(35):e0054521. doi: 10.1128/MRA.00545-21

14. Huang Y, Niu B, Gao Y, Fu L, Li W. CD-HIT Suite: a web server for clustering and comparing biological sequences. *Bioinf (Oxford England)* (2010) 26(5):680–2. doi: 10.1093/bioinformatics/btq003

15. Luo H, Lin Y, Gao F, Zhang C-T, Zhang R. DEG 10, an update of the database of essential genes that includes both protein-coding genes and noncoding genomic elements. *Nucleic Acids Res* (2014) 42(D1):D574–80. doi: 10.1093/nar/gkt1131

16. Johnson M, Zaretskaya I, Raytselis Y, Merezhuk Y, McGinnis S, Madden TL. NCBI BLAST: a better web interface. *Nucleic Acids Res* (2008) 36(suppl_2):W5–9. doi: 10.1093/nar/gkn201

17. Sayers EW, Agarwala R, Bolton EE, Brister JR, Canese K, Clark K, et al. Database resources of the national center for biotechnology information. *Nucleic Acids Res* (2019) 47(D1):D23–8. doi: 10.1093/nar/gky1069

18. Coordinators NR. Database resources of the national center for biotechnology information. *Nucleic Acids Res* (2013) 41(D1):D8–D20. doi: 10.1093/nar/gkx1095

19. Gupta R, Pradhan D, Jain AK, Rai CS. TiD: Standalone software for mining putative drug targets from bacterial proteome. *Genomics* (2017) 109(1):51–7. doi: 10.1016/j.ygeno.2016.11.005

20. Yu NY, Wagner JR, Laird MR, Melli G, Rey S, Lo R, et al. PSORTb 3.0: improved protein subcellular localization prediction with refined localization subcategories and predictive capabilities for all prokaryotes. *Bioinf (Oxford England)* (2010) 26(13):1608–15. doi: 10.1093/bioinformatics/btq249

21. Saha S, Raghava GP. Prediction of continuous B-cell epitopes in an antigen using recurrent neural network. *Proteins* (2006) 65(1):40–8. doi: 10.1002/prot.21078

22. Fleri W, Paul S, Dhanda SK, Mahajan S, Xu X, Peters B, et al. The immune epitope database and analysis resource in epitope discovery and synthetic vaccine design. *J Front Immunol* (2017) 8(278):278. doi: 10.3389/fimmu.2017.00278

23. Doytchinova IA, Flower DR. VaxiJen: a server for prediction of protective antigens, tumour antigens and subunit vaccines. *BMC Bioinf* (2007) 8:4. doi: 10.1186/1471-2105-8-4

24. Dimitrov I, Flower DR, Doytchinova I. AllerTOP–a server for in silico prediction of allergens. *BMC Bioinf* (2013) 14 Suppl6(Suppl 6):S4. doi: 10.1186/1471-2105-14-S6-S4

25. Gupta S, Kapoor P, Chaudhary K, Gautam A, Kumar ROpen Source Drug Discovery C, et al. In silico approach for predicting toxicity of peptides and proteins. *PloS One* (2013) 8(9):e73957. doi: 10.1371/journal.pone.0073957

26. Bui HH, Sidney J, Dinh K, Southwood S, Newman MJ, Sette A. Predicting population coverage of T-cell epitope-based diagnostics and vaccines. *BMC Bioinf* (2006) 7:153. doi: 10.1186/1471-2105-7-153

27. Rahman N, Ali F, Basharat Z, Shehroz M, Khan MK, Jeandet P, et al. Vaccine design from the ensemble of surface glycoprotein epitopes of SARS-CoV-2: An immunoinformatics approach. *Vaccines* (2020) 8(3):423. doi: 10.3390/vaccines8030423

28. Nezafat N, Karimi Z, Eslami M, Mohkam M, Zandian S, Ghasemi Y. Designing an efficient multi-epitope peptide vaccine against Vibrio cholerae via combined immunoinformatics and protein interaction based approaches. *Comput Biol Chem* (2016) 62:82–95. doi: 10.1016/j.compbiolchem.2016.04.006

29. Aiman S, Ali F, Zia A, Aslam M, Han Z, Shams S, et al. Core genome mediated potential vaccine targets prioritization against Clostridium difficile via reverse vaccinology-an immuno-informatics approach. *JJoBR-T* (2022) 29. doi: 10.26262/jbrt.v29i0.8481

30. Solanki V, Tiwari V. Subtractive proteomics to identify novel drug targets and reverse vaccinology for the development of chimeric vaccine against Acinetobacter baumannii. *Sci Rep* (2018) 8(1):9044. doi: 10.1038/s41598-018-26689-7

31. Wilkins MR, Gasteiger E, Bairoch A, Sanchez JC, Williams KL, Appel RD, et al. Protein identification and analysis tools in the ExPASy server. *Methods Mol Biol (Clifton NJ)* (1999) 112:531–52. doi: 10.1385/1-59259-584-7:531

32. Magnan CN, Randall A, Baldi P. SOLpro: accurate sequence-based prediction of protein solubility. *Bioinf (Oxford England)* (2009) 25(17):2200–7. doi: 10.1093/bioinformatics/btp386

33. Cheng J, Randall AZ, Sweredoski MJ, Baldi P. SCRATCH: a protein structure and structural feature prediction server. *Nucleic Acids Res* (2005) 33(suppl_2):W72–6. doi: 10.1093/nar/gki396

34. Buchan DWA, Jones DT. The PSIPRED Protein Analysis Workbench: 20 years on. *Nucleic Acids Res* (2019) 47(W1):W402–7. doi: 10.1093/nar/gkz297

35. Geourjon C, Deléage G. SOPMA: significant improvements in protein secondary structure prediction by consensus prediction from multiple alignments. *Comput Appl Biosci* (1995) 11(6):681–4. doi: 10.1093/bioinformatics/11.6.681

36. Kelley LA, Mezulis S, Yates CM, Wass MN, Sternberg MJE. The Phyre2 web portal for protein modeling, prediction and analysis. *Nat Protoc* (2015) 10(6):845–58. doi: 10.1038/nprot.2015.053

37. Heo L, Park H, Seok C. GalaxyRefine: Protein structure refinement driven by side-chain repacking. *Nucleic Acids Res* (2013) 41(Web Server issue):W384–388. doi: 10.1093/nar/gkt458

38. Lovell SC, Davis IW, Arendall Iii WB, de Bakker PIW, Word JM, Prisant MG, et al. Structure validation by Cα geometry: ϕ,ψ and Cβ deviation. *Proteins: Structure Function Bioinf* (2003) 50(3):437–50. doi: 10.1002/prot.10286

39. Wiederstein M, Sippl MJ. ProSA-web: interactive web service for the recognition of errors in three-dimensional structures of proteins. *Nucleic Acids Res* (2007) 35(Web Server issue):W407–410. doi: 10.1093/nar/gkm290

40. Ponomarenko J, Bui HH, Li W, Fusseder N, Bourne PE, Sette A, et al. ElliPro: a new structure-based tool for the prediction of antibody epitopes. *BMC Bioinf* (2008) 9:514. doi: 10.1186/1471-2105-9-514

41. Kozakov D, Hall DR, Xia B, Porter KA, Padhorny D, Yueh C, et al. The ClusPro web server for protein–protein docking. *Nat Protoc* (2017) 12(2):255–78. doi: 10.1038/nprot.2016.169

42. Laskowski RA, Jabłońska J, Pravda L, Vařeková RS, Thornton JM. PDBsum: Structural summaries of PDB entries. *Protein Sci* (2018) 27(1):129–34. doi: 10.1002/pro.3289

43. López-Blanco JR, Aliaga JI, Quintana-Ortí ES, Chacón P. iMODS: internal coordinates normal mode analysis server. *Nucleic Acids Res* (2014) 42(Web Server issue):W271–276. doi: 10.1093/nar/gku339

44. Bowers KJ, Chow E, Xu H, Dror RO, Eastwood MP, Gregersen BA, et al. (2006). Scalable algorithms for molecular dynamics simulations on commodity clusters, in: *Proceedings of the 2006 ACM/IEEE conference on Supercomputing*, Tampa, Florida: Association for Computing Machinery. pp. 84–es.

45. Lu C, Wu C, Ghoreishi D, Chen W, Wang L, Damm W, et al. OPLS4: improving force field accuracy on challenging regimes of chemical space. *J Chem Theory Comput* (2021) 17(7):4291–300. doi: 10.1021/acs.jctc.1c00302

46. Jorgensen W, Chandrasekhar J, Madura J, Impey R, Klein M. Comparison of simple potential functions for simulating liquid water. *J Chem Phys* (1983) 79:926–35. doi: 10.1063/1.445869

47. Kräutler V, van Gunsteren WF, Hünenberger PH. A fast SHAKE algorithm to solve distance constraint equations for small molecules in molecular dynamics simulations. *J Comput Chem* (2001) 22(5):501–8. doi: 10.1002/1096-987X(20010415)22:5<501::AID-JCC1021>3.0.CO;2-V

48. Bakan A, Meireles LM, Bahar I. ProDy: protein dynamics inferred from theory and experiments. *Bioinf (Oxford England)* (2011) 27(11):1575–7. doi: 10.1093/bioinformatics/btr168

49. Rapin N, Lund O, Bernaschi M, Castiglione F. Computational immunology meets bioinformatics: the use of prediction tools for molecular binding in the simulation of the immune system. *PloS One* (2010) 5(4):e9862. doi: 10.1371/journal.pone.0009862

50. Nain Z, Abdulla F, Rahman MM, Karim MM, Khan MSA, Sayed SB, et al. Proteome-wide screening for designing a multi-epitope vaccine against emerging pathogen Elizabethkingia anophelis using immunoinformatic approaches. *J Biomolecular Structure Dynamics* (2020) 38(16):4850–67. doi: 10.1080/07391102.2019.1692072

51. Ezeanolue E, Harriman K, Hunter P, Kroger A, Pellegrini C. General best practice guidelines for immunization: best practices guidance of the Advisory Committee on Immunization Practices (ACIP). *Natl Center Immunization Respir Dis* (2019).

52. Grote A, Hiller K, Scheer M, Münch R, Nörtemann B, Hempel DC, et al. JCat: a novel tool to adapt codon usage of a target gene to its potential expression host. *Nucleic Acids Res* (2005) 33(Web Server issue):W526–31. doi: 10.1093/nar/gki376

53. Ismail S, Abbasi SW, Yousaf M, Ahmad S, Muhammad K, Waheed Y. Design of a multi-epitopes vaccine against hantaviruses: an immunoinformatics and molecular modelling approach. *Vaccines (Basel)* (2022) 10(3):378. doi: 10.3390/vaccines10030378

54. Manning PA, Heuzenroeder MW, Yeadon J, Leavesley DI, Reeves PR, Rowley D. Molecular cloning and expression in Escherichia coli K-12 of the O antigens of the Inaba and Ogawa serotypes of the Vibrio cholerae O1 lipopolysaccharides and their potential for vaccine development. *Infection Immun* (1986) 53(2):272–7. doi: 10.1128/iai.53.2.272-277.1986

55. Kamens J. The Addgene repository: an international nonprofit plasmid and data resource. *Nucleic Acids Res* (2015) 43(D1):D1152–7. doi: 10.1093/nar/gku893

56. Kalesh K, Wei W, Mantilla BS, Roumeliotis TI, Choudhary J, Denny PW. Transcriptome-wide identification of coding and noncoding RNA-binding proteins defines the comprehensive RNA interactome of leishmania mexicana. *Microbiol Spectr* (2022) 10(1):e0242221. doi: 10.1128/spectrum.02422-21

57. Alonso A, Larraga J, Loayza FJ, Martínez E, Valladares B, Larraga V, et al. Stable episomal transfectant leishmania infantum promastigotes over-expressing the DEVH1 RNA helicase gene down-regulate parasite survival genes. *Pathog (Basel Switzerland)* (2022) 11(7):761. doi: 10.3390/pathogens11070761

58. Kutateladze TG. Phosphatidylinositol 3-phosphate recognition and membrane docking by the FYVE domain. *Biochim Biophys Acta* (2006) 1761(8):868–77. doi: 10.1016/j.bbalip.2006.03.011

59. Andrade JM, Gonçalves LO, Liarte DB, Lima DA, Guimarães FG, de Melo Resende D, et al. Comparative transcriptomic analysis of antimony resistant and susceptible Leishmania infantum lines. *Parasites Vectors* (2020) 13(1):600. doi: 10.1186/s13071-020-04486-4

60. Wu C-Y, Monie A, Pang X, Hung C-F, Wu TC. Improving therapeutic HPV peptide-based vaccine potency by enhancing CD4+ T help and dendritic cell activation. *J Biomed Sci* (2010) 17(1):88. doi: 10.1186/1423-0127-17-88

61. Kropf P, Freudenberg MA, Modolell M, Price HP, Herath S, Antoniazi S, et al. Toll-like receptor 4 contributes to efficient control of infection with the protozoan parasite Leishmania major. *Infection Immun* (2004) 72(4):1920–8. doi: 10.1128/IAI.72.4.1920-1928.2004

62. Aguirre-García MM, Araceli R-B, Gómez-García AP, Alma RE-M. TLR-mediated host immune response to parasitic infectious diseases. In: Nima R, editor. *Toll-like Receptors*. Rijeka: IntechOpen (2019). Ch. 3.

63. Carvalho LH, Sano G, Hafalla JC, Morrot A, Curotto de Lafaille MA, Zavala F. IL-4-secreting CD4+ T cells are crucial to the development of CD8+ T-cell responses against malaria liver stages. *Nat Med* (2002) 8(2):166–70. doi: 10.1038/nm0202-166

64. Clem AS. Fundamentals of vaccine immunology. *J Global Infect Dis* (2011) 3(1):73–8. doi: 10.4103/0974-777X.77299

65. Hoque MN, Istiaq A, Clement RA, Sultana M, Crandall KA, Siddiki AZ, et al. Metagenomic deep sequencing reveals association of microbiome signature with functional biases in bovine mastitis. *Sci Rep* (2019) 9(1):13536. doi: 10.1038/s41598-019-49468-4

66. Wang C, Yang S, Duan L, Du X, Tao J, Wang Y, et al. Adaptive immune responses and cytokine immune profiles in humans following prime and boost vaccination with the SARS-CoV-2 CoronaVac vaccine. *Virol J* (2022) 19(1):223. doi: 10.1186/s12985-022-01957-1

67. Kaminski GA, Friesner RA, Tirado-Rives J, Jorgensen WL. Evaluation and reparametrization of the OPLS-AA force field for proteins via comparison with accurate quantum chemical calculations on peptides. *J Phys Chem B* (2001) 105(28):6474–87. doi: 10.1021/jp003919d

68. Zhang J, Shi Z, Kong FK, Jex E, Huang Z, Watt JM, et al. Topical application of Escherichia coli-vectored vaccine as a simple method for eliciting protective immunity. *Infection Immun* (2006) 74(6):3607–17. doi: 10.1128/IAI.01836-05

69. Kakakhel S, Ahmad A, Mahdi WA, Alshehri S, Aiman S, Begum S, et al. Annotation of Potential Vaccine Targets and Designing of mRNA-Based Multi-Epitope Vaccine against Lumpy Skin Disease Virus via Reverse Vaccinology and Agent-Based Modeling. *Bioengineering* (2023) 10:430. doi: 10.3390/bioengineering10040430

70. Aiman S, Alhamhoom Y, Ali F, Rahman N, Rastrelli L, Khan A, et al. Multi-epitope chimeric vaccine design against emerging Monkeypox virus via reverse vaccinology techniques- a bioinformatics and immunoinformatics approach. *Front Immunol* (2022) 13:985450. doi: 10.3389/fimmu.2022.985450

71. Malvolti S, Malhame M, Mantel CF, Le Rutte EA, Kaye PM. Human leishmaniasis vaccines: Use cases, target population and potential global demand. *PloS Negl Trop Dis* (2021) 15(9):e0009742. doi: 10.1371/journal.pntd.0009742

72. John L, John GJ, Kholia T. A reverse vaccinology approach for the identification of potential vaccine candidates from leishmania spp. *Appl Biochem Biotechnol* (2012) 167(5):1340–50. doi: 10.1007/s12010-012-9649-0

73. Dikhit MR, Sen A. Elucidation of conserved multi-epitope vaccine against Leishmania donovani using reverse vaccinology. *J biomolecular structure dynamics* (2023) 2023:1–14. doi: 10.1080/07391102.2023.2201630

74. Gouda AM, Soltan MA, Abd-Elghany K, Sileem AE, Elnahas HM, Ateya MA, et al. Integration of immunoinformatics and cheminformatics to design and evaluate a multitope vaccine against Klebsiella pneumoniae and Pseudomonas aeruginosa coinfection. *Front Mol Biosci* (2023) 10:1123411. doi: 10.3389/fmolb.2023.1123411

75. Arpin C, Déchanet J, Van Kooten C, Merville P, Grouard G, Brière F, et al. Generation of memory B cells and plasma cells. *vitro. Sci (New York NY)* (1995) 268 (5211):720–2. doi: 10.1126/science.7537388

76. Bacchetta R, Gregori S, Roncarolo MG. CD4+ regulatory T cells: mechanisms of induction and effector function. *Autoimmun Rev* (2005) 4(8):491–6. doi: 10.1016/j.autrev.2005.04.005

77. Jalal K, Khan K, Basharat Z, Abbas MN, Uddin R, Ali F, et al. Reverse vaccinology approach for multi-epitope centered vaccine design against delta variant of the SARS-CoV-2. *Environ Sci pollut Res Int* (2022) 29(40):60035–53. doi: 10.1007/s11356-022-19979-1

78. Li J, Qiu J, Huang Z, Liu T, Pan J, Zhang Q, et al. Reverse vaccinology approach for the identifications of potential vaccine candidates against Salmonella. *Int J Med Microbiol* (2021) 311(5):151508. doi: 10.1016/j.ijmm.2021.151508

79. Guedes RLM, Rodrigues CMF, Coatnoan N, Cosson A, Cadioli FA, Garcia HA, et al. A comparative in silico linear B-cell epitope prediction and characterization for South American and African Trypanosoma vivax strains. *Genomics* (2019) 111(3):407–17. doi: 10.1016/j.ygeno.2018.02.017

80. Hasan M, Azim KF, Begum A, Khan NA, Shammi TS, Imran AS, et al. Vaccinomics strategy for developing a unique multi-epitope monovalent vaccine against Marburg marburgvirus. *Infect Genet Evol* (2019) 70:140–57. doi: 10.1016/j.meegid.2019.03.003

81. Bazhan SI, Antonets DV, Karpenko LI, Oreshkova SF, Kaplina ON, Starostina EV, et al. In silico designed ebola virus T-cell multi-epitope DNA vaccine constructions are immunogenic in mice. *Vaccines (Basel)* (2019) 7(2):1–34. doi: 10.3390/vaccines7020034

82. Carneiro PP, Dórea AS, Oliveira WN, Guimarães LH, Brodskyn C, Carvalho EM, et al. Blockade of TLR2 and TLR4 attenuates inflammatory response and parasite load in cutaneous leishmaniasis. *Front Immunol* (2021) 12:706510. doi: 10.3389/fimmu.2021.706510

83. Aiman S, Ali Y, Malik A, Alkholief M, Ahmad A, Akhtar S, et al. Immunoinformatic-guided novel mRNA vaccine designing to elicit immunogenic responses against the endemic Monkeypox virus. *J Biomolecular Structure Dynamics* (2023) 2023:1–15. doi: 10.1080/07391102.2023.2233627

84. Jalal K, Khan K, Basharat Z, Abbas MN, Uddin R, Ali F, et al. Hassan SSu: Reverse vaccinology approach for multi-epitope centered vaccine design against delta variant of the SARS-CoV-2. *Environ Sci pollut Res* (2022) 29(40):60035–53. doi: 10.1007/s11356-022-19979-1

85. Enayatkhani M, Hasaniazad M, Faezi S, Gouklani H, Davoodian P, Ahmadi N, et al. Reverse vaccinology approach to design a novel multi-epitope vaccine candidate against COVID-19: an in silico study. *J biomolecular structure dynamics* (2021) 39 (8):2857–72. doi: 10.1080/07391102.2020.1756411

86. Alsowayeh N, Albutti A, Al-Shouli ST. Reverse vaccinology and immunoinformatic assisted designing of a multi-epitopes based vaccine against nosocomial burkholderia cepacia. *Front Microbiol* (2022) 13:929400. doi: 10.3389/fmicb.2022.929400

87. Ren S, Guan L, Dong Y, Wang C, Feng L, Xie Y. Design and evaluation of a multi-epitope assembly peptide vaccine against Acinetobacter baumannii infection in mice. *Swiss Med Wkly* (2019) 149:w20052. doi: 10.4414/smw.2019.20052

88. Stolfi P, Castiglione F, Mastrostefano E, Di Biase I, Di Biase S, Palmieri G, et al. In-silico evaluation of adenoviral COVID-19 vaccination protocols: Assessment of immunological memory up to 6 months after the third dose. *Front Immunol* (2022) 13:998262. doi: 10.3389/fimmu.2022.998262

89. Concetta R, Carmen M, Beatrice C, Angela M, Maria Lina T, Franco MB, et al. Identification and validation of viral antigens sharing sequence and structural homology with tumor-associated antigens (TAAs). *J ImmunoTherapy Cancer* (2021) 9(5):e002694. doi: 10.1016/j.ejca.2018.12.022

90. Farzan M, Farzan M, Mirzaei Y, Aiman S, Azadegan-Dehkordi F, Bagheri N. Immunoinformatics-based multi-epitope vaccine design for the re-emerging monkeypox virus. *Int Immunopharmacol* (2023) 123:110725. doi: 10.1016/j.intimp.2023.110725

91. Aslam M, Shehroz M, Ali F, Zia A, Pervaiz S, Shah M, et al. Chlamydia trachomatis core genome data mining for promising novel drug targets and chimeric vaccine candidates identification. *Comput Biol Med* (2021) 136:104701. doi: 10.1016/j.compbiomed.2021.104701

92. Aslam M, Shehroz M, Hizbullah, Shah M, Khan MA, Afridi SG, et al. Potential druggable proteins and chimeric vaccine construct prioritization against Brucella melitensis from species core genome data. *Genomics* (2020) 112(2):1734–45. doi: 10.1016/j.ygeno.2019.10.009